FRACTURE BEHAVIOR OF TYRANNO-ZMI FIBER EXPOSED IN AIR AT 1173 ~ 1673 K

K.Morishita[1], M.Hojo[1], H.Okuda[2], S.Ochiai[2], M.Sato[3]

[1]Department of Materials Science and Engineering, Kyoto University, Yoshida, Sakyo-ku, Kyoto 606-8501, Japan
[2]International Innovation Center, Kyoto University, Yoshida, Sakyo-ku, Kyoto 606-8501, Japan
[3]Ube Research Laboratory, Ube Industries Ltd, 1978-5 Koguchi, Ube city, Yamaguchi 755-8633, Japan

ABSTRACT

The fracture behavior of the Tyranno-ZMI fiber exposed in air at 1173 ~ 1673K for 2×10^4s was studied. The average strength of the fiber with SiO_2 layer on its surface decreased and the scatter of strength increased with increasing exposure temperature. The fracture of the fiber was controlled by the propagation of the crack made by the premature fracture of the SiO_2 layer into fiber. The average strength of the fiber without SiO_2 layer prepared by etching away the SiO_2 layer from the fiber exposed in air, decreased also with increasing exposure temperature, whereas it was far higher than that of the fiber with SiO_2 layer. The fracture toughness of the fiber, which was originally amorphous decreased with increasing exposure temperature due to the crystallization. In this way, the high temperature-exposure in air caused degradation of the fiber itself and the SiO_2 layer-originated crack propagation.

1 INTRODUCTION

SiC/SiC composites are attractive candidates as materials for advanced energy system, such as high performance combustion systems, which are used in severe conditions (high temperature, high loading and long duration) (Kohyama [1]). It is needed to reveal the mechanical and oxidation resistance of these composites for application.

Heat resistance of SiC fibers depends on the amount of oygen content introduced in curing process (Johnson [2], Shimoo [3], Vahlas [4]). The oxidation-cured SiC fibers, such as Nicalon and Tyranno-LoxM with relatively high oxygen content, have low heat resistance. On the contrary, Tyranno-ZMI with slightly lower oxygen content has higher heat resistance than them. Thus, Tyranno-ZMI is one of the most attractive candidates for reinforcement.

It is well known when the fibers is exposed in air, the oxidation progresses. In this progress, the SiO_2 layer retards the progress of oxidation on fiber surface due to the passive nature (Kakimoto [5]). Nevertheless, the degradation of the fiber by oxidation has been reported (Yamaoka [6]), while the degradation mechanism has not been clarified yet.

The aim of the present work is to clarify the fracture mechanism of Tyranno-ZMI fibers exposed at high temperatures in air. For this aim, we measured tensile strength and observed fracture morphology and microstructure for Tyranno-ZMI fibers exposed in air at 1173 ~ 1673K. Then we discussed the results from the fracture mechanical view point.

2 EXPERIMENTAL PROCEDURE

The Tyranno-ZMI (hereafter noted as the fiber for convenience) fiber used for the present study had the composition $SiZr_{<0.01}C_{1.44}O_{0.32}$ and the mean diameter 11μm. This fiber was produced by Ube Industries [7]. The fiber has mostly amorphous structure, in which the β-SiC crystals in the form of 2nm particles exist in amorphous phase (Yamaoka [6]).

The fiber-specimens, whose sizing agent had already been removed by the heat treatment in air at 873 K for 1.8×10^3 s, were exposed in air at 1173,1473 and 1673 K for 2×10^4 s.

To investigate the products generated by the air-exposure at the temperatures stated above, the specimens were examined by powder X-ray diffraction method (RINT2200, Rigaku).

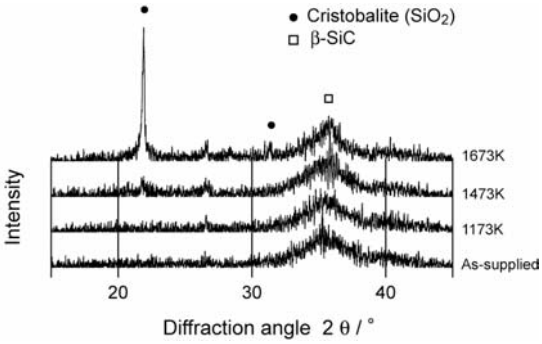

Fig.1 X-ray diffraction patterns for the Tyranno-ZMI fiber as-supplied and exposed in air at 1173, 1473 and 1673K for 20ks.

As shown later in 3.1, the SiO_2 layer formed on the surface of the fiber. In order to detect the influence of the SiO_2 layer, the fibers with and without SiO_2 layer were tested. The fiber without SiO_2 layer was prepared by etching away the SiO_2 with HF + NH_4F (5:1 molar ratio) solution at 303 K for 1.8×10^3 s.

Tensile test of the as-supplied, exposed (with SiO_2 layer) and etched after exposure (without SiO_2 layer) monofilament fibers was carried out at room temperature at a crosshead speed of 8.3×10^{-6} m/s for a gage length 20mm, with a universal tensile testing machine (MMT-10N-2, Shimadzu, load cell 2.5N). The fracture surface and the appearance of the side surface were observed with FE-SEM (Field Emission Scanning Electron Microscope) (X-900, Hitachi) without conductive coating.

3 RESULTS AND DISCUSSIONS

3.1.Strength of fiber

X-ray diffraction patterns of the fibers as-supplied and exposed in air for 20 ks at 1173 ~ 1673 K are shown in Fig.1. The peak at a diffraction angle of $2\theta \cong 22$ degree corresponds to the cristobalite of the SiO_2, which formed on the fiber surface when exposed above 1473 K, and it grew with increasing exposure temperature. The amorphous SiO_2 was not detected by this method, but formed at 1173K and degraded the property as shown later.

Figure 2 shows the measured tensile strength of the ZMI fibers plotted against exposure temperature, T .

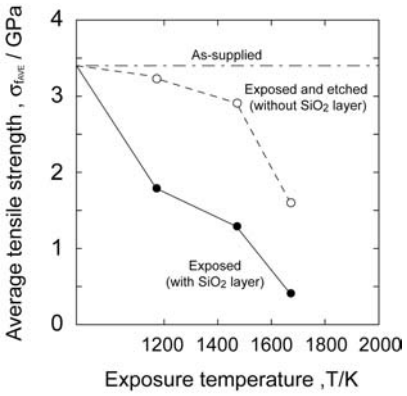

Fig.2 Tensile strength of the Tyranno-ZMI fiber exposed in air at 1173, 1473 and 1673K for 20ks.

According to the Weibull distribution function (Weibull [8]), the cumulative probability of failure F at a stress σ_f for the fiber with a length L is given by

$$F = 1 - \left\{ -\left(L / L_0\right)\left(\sigma_f / \sigma_0\right)^m \right\} \quad (1)$$

where m and σ_0 are the shape and scale parameters, respectively, and L_0 is the standard length, which was taken to be equal to L in this work. Figure 3 shows the result of the Weibull plot (the plot of $\ln\ln\left(1-F\right)^{-1}$ against $\ln\left(\sigma_f\right)$). From the slope and extrapolation, the m and σ_0 values were estimated, respectively. The estimated values are presented in Table 1, together with the average strength. The measured strength-distributions of the fibers and the calculated ones with the estimated m and σ_0 values are presented in Fig.4. The following features were read from Table 1 and Figs.2, 3 and 4.

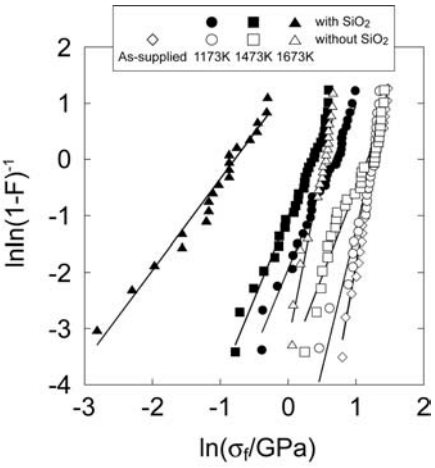

Fig.3 Weibull plot for the measured fiber strength σ_f. ●, ■ and ▲ has the SiO_2 layer formed on the fiber surface, and the other has no SiO_2 layer.

(1) The average strength of the as-supplied fibers was 3.41 GPa. The average strength of the fibers with SiO_2 layer (●) decreased with increasing exposure temperature; 1.79, 1.29 and 0.41 GPa for exposure at 1173, 1473 and 1673 K. The degradation ratio (1 − strength of exposed fiber / strength of as-supplied fiber) was 54, 67 and 89 %, respectively.

(2) Concerning the difference in strength between the exposed (with SiO_2 layer) (●) and etched

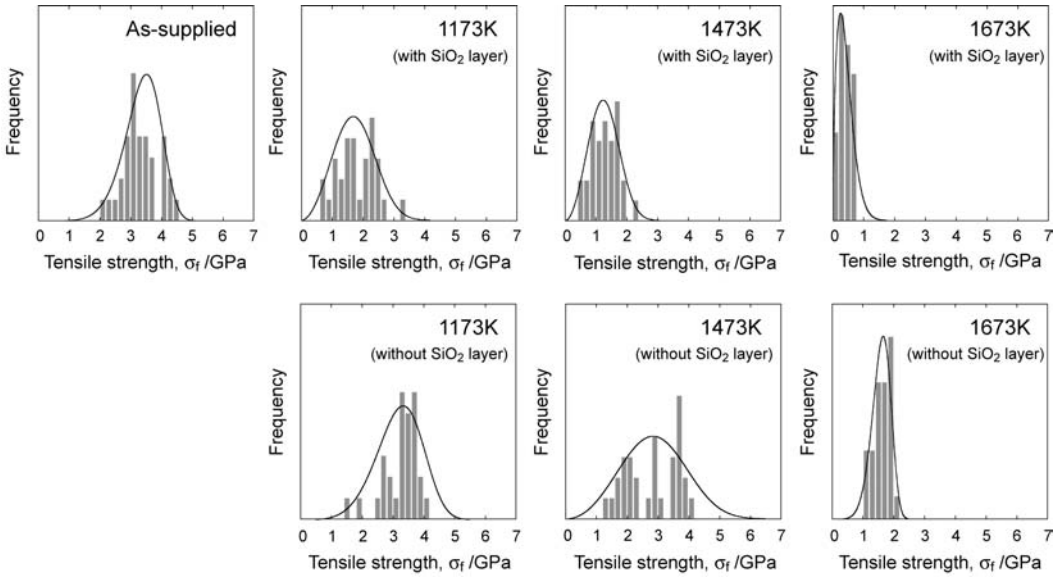

Fig.4 Distribution of the tensile strength of Tyranno-ZMI fiber as-supplied, exposed (with SiO_2 layer) and etched (without SiO_2 layer), and each Weibull distribution function estimated from Fig.3 and Table 1.

(without SiO_2 layer) (○) fibers, the strength of the former fiber was far lower than that of the latter one. It has been reported that the origin of the fracture of the ZMI fibers exposed in air is the premature cracking of the SiO_2 layer and extension of such a crack into fibers (Ochiai [9]). In this fracture mechanism, the fiber strength decreases with increasing thickness of the SiO_2 layer [9]. This suggests that the strength of fibers without SiO_2 layer will become far higher than the strength level of the fiber with SiO_2 layer. As shown in Fig.2, the measured tensile strength of SiO_2-removed fibers was actually far higher than that of fibers with SiO_2 layer below the exposure temperature 1673 K, showing that the existent SiO_2 layer actually caused fiber fracture. The reason for the reduction in the etched fibers will be discussed later in 3.3.

(3) The higher the exposure temperature, the lower became the Weibull shape parameter. There was a strong correlation between the tensile strength and the Weibull's shape parameter for the fiber with SiO_2; the lower the strength , the smaller became the scale parameter.

Table 1 Results of tensile test of the fibers.

	as-supplied	Exposure temperature (K)					
		1173		1473		1673	
		with SiO_2	without SiO_2	with SiO_2	without SiO_2	with SiO_2	without SiO_2
Average strength, $\sigma_{f,AVE}$ (GPa)	3.41	1.79	3.23	1.29	2.91	0.41	1.60
Shape parameter, m	6.69	2.91	4.97	2.91	3.10	1.62	6.07
Scale parameter, σ_0 (GPa)	3.61	1.95	3.50	1.95	3.50	0.46	1.70

3.2. Morphology

The appearance of the fiber exposed in air at 1473 and 1673K for 20ks is shown in Fig.5. (a) shows the applied stress-induced circumferential cracks of the SiO_2 layer. (b) shows the fracture surface of the fiber exposed at 1673 K. Judging from the fracture path accompanied by the mirror and mist zones, the fracture of the fiber originated from the SiO_2 layer. This fracture pattern indicates that the strength of the fiber with SiO_2 is controlled by the oxide layer. (c) ~ (f) show the side surface of the fiber itself. Among them, (c) and (d) show the side surface of the fiber exposed at 1473 K and then etched, observed at low and high magnifications, respectively. (e) and (f) show the side surface of the fiber exposed at 1673 K and then etched, observed at low and high magnifications, respectively. In the case of 1473 K exposure, the side surface of the fiber itself was very smooth. On the other hand, in the case of 1673 K exposure, the surface was not smooth but rough. This implies that the structure of the fiber changed. The reduction in strength of the fiber without SiO_2 layer (3 GPa for 1473 K-exposure to 1 GPa for 1673 K-exposure in Fig.2) could be attributed to such a structural change due to the crystallization, as will be discussed below.

3.3. Estimation of the fracture toughness of the fiber exposed in air at high temperatures

As stated already, the fracture mechanism of the fiber exposed in air at high temperatures is the propagation of the crack made by the premature fracture of SiO_2 layer on fiber surface. Thus the size of the strength-determing crack could be regarded as the thickness of the SiO_2 layer, as schematically shown in Fig.6. Applying the shorshorove's approximation [10], the critical stress intensity factor K_{Ic} could be approximately expressed in the form

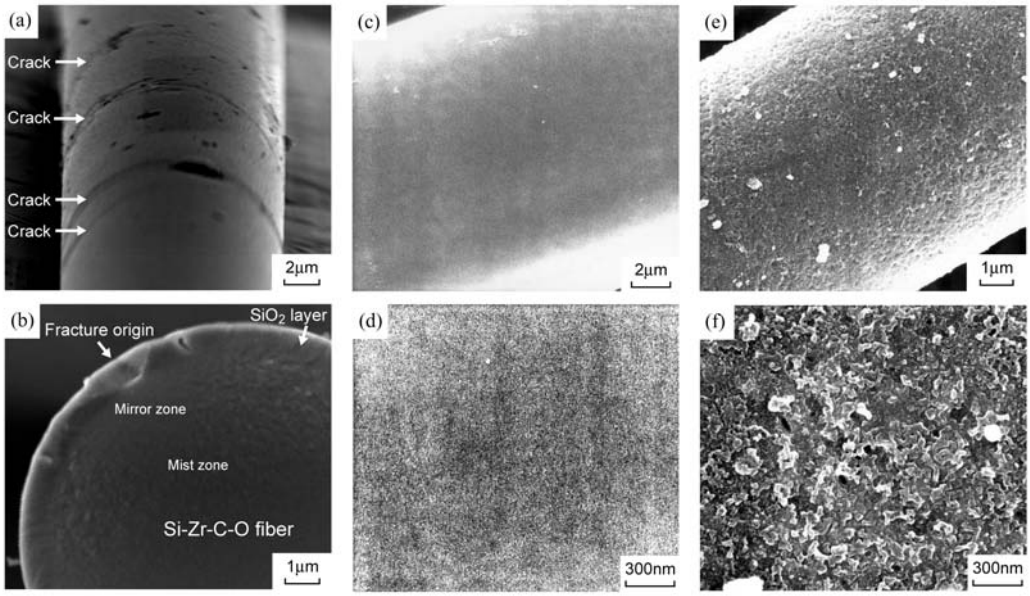

Fig.5 The morphology of the fiber exposed in air at 1473 and 1673 K for 20 ks. (a): Circumferential crack of SiO_2 layer under applied stress. (b): Fracture surface of the fiber exposed at 1673 K. (c) and (d) : Side surface of the fiber itself after exposure at 1473 K. (e) and (f): Side surface of the fiber itself after exposure at 1673 K.

$$K_{Ic} = \sqrt{\frac{E_{\mathrm{SiO_2}}}{E_{\mathrm{f}}}} \cdot \sigma_{\mathrm{f,net}} \sqrt{\pi(b-a) \cdot a/b} \cdot G\left(a/b\right) \tag{2}$$

where E_{f} and E_{SiO2} are the Young's modulus of the fiber and the SiO_2 layer being 200 and 72 GPa, respectively. $\sigma_{\mathrm{f,net}}$ is the net strength of fiber (=the load at fracture / cross-sectional area of the fiber (πa^2)). $2a$ and $2b$ are the diameter of the fiber itself and that of the overall SiO_2 coated-fiber, respectively, and $G(a/b)$ is the finite width correction factor. Substituting the measured values of a =5.70, b =6.37 μm and $\sigma_{\mathrm{f,net}}$ =1.62 GPa for 1473K exposure, and a =5.58, b =6.40 μm and $\sigma_{\mathrm{f,net}}$ =0.54 GPa for 1673K exposure into Eq(2), the critical stress intensity factor of the fiber exposed at 1473 and 1673K was estimated to be 1.30 and 0.77 MPa$\sqrt{\mathrm{m}}$, respectively. Until now, the K_{Ic} values of the Si-C-O(Nicalon) and Si-Ti-C-O(Tyranno-LoxM) fiber have been reported to be 1 (Kondo [11]) and 1.4 (Matsunaga [12]) MPa$\sqrt{\mathrm{m}}$, respectively. The estimated K_{Ic} value of the present ZMI fiber exposed at 1473K was similar to such values, while the value for 1673K exposure was lower than them. As stated already, the structure of the fiber changed from 1473 to 1673K air exposure (Fig.5). It has been reported that β-SiC

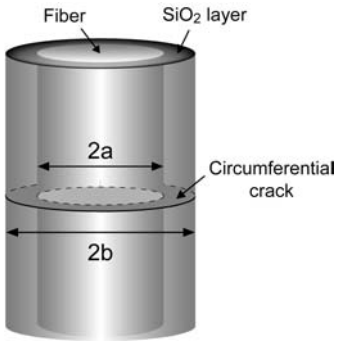

Fig.6 Schematic representation of notched material for estimation of K_{Ic}.

grain grows with increasing exposure temperature [6]. The reduction in K_{Ic} for 1673K exposure in comparison with that for 1473K exposure could be attributed to the structural change of the fiber itself. Such a structural change-induced reduction in K_{Ic} could be mentioned as one of the reasons to cause severe reduction of fiber itself for 1673K exposure.

4 CONCLUSIONS

The fracture behavior of the Tyranno-ZMI fiber exposed in air at 1173 ~ 1673 K for 2×10^4 s was studied. The average strength of the fiber decreased the scatter of strength increased with increasing exposure temperature. The fracture of the exposed fiber was controlled by the propagation of the crack made by the premature fracture of the SiO_2 layer into fiber. The fracture toughness of the fiber decreased with increasing exposure temperature. The increase in thickness of the SiO_2 layer and decrease in fracture toughness of the fiber due to the crystallization resulted in severe reduction in fiber strength at high temperature exposure in air.

ACKNOWLEDGEMENTS

The present work was supported by the New Energy and Industrial Technology Development Organization (NEDO), Japan

REFERENCES

1. Kohyama A and Katoh Y, Advanced SiC/SiC ceramic composites: developments and applications in energy systems. Ceram Trans, 144, 3-18, 2002.
2. Johnson M, Britten R.D, Lamoreaux R.H. and Rowcliff D.J, J. Amer. Ceram. Soc., 71, C-132, 1988.
3. Shimoo T, Sugimoto M and Okamura K, J. Jpn. Inst. Metals, 54, 802, 1990.
4. Vahlas C, Rocabois P and Bernard C, J. Mater. Sci., 29, 5839, 1994.
5. Kakimoto K, Kakehi Y, Shimoo T and Okamura K, J. Jpn. Soc. Powder and Powder Metallurgy, 39, 451-454, 1992.
6. Yamaoka H, Shibuya M, Kumagawa K and Okamura K, J. Ceram. Soc. Japan, 109-3, 217-221, 2001.
7. Yamaoka H, Ishikawa T and Kumagawa K, J. Mater. Sci., 34, 1333-1339, 1999.
8. Weibull W., J.Appl.Phys.,18, 293-297, 1951.
9. Ochiai S, Kimura S, Tanaka H, Tanaka M, Hojo M, Morishita K, Okuda H, Nakayama H, Tamura M, Shibata K and Sato M, Composites PartA, 35, 41-50, 2004.
10. Shorshorov M.K, Ustinov L.M, Zirlin A.M, Olefilebko VL, Vonogradov LV, J. Mater. Sci., 14, 1850-1861, 1979.
11. Kondo M, Imai Y, Tezuka H and Kohyama A, Testu-to-Hagane, 75, 1463-1469, 1989.
12. Matsunaga K, Ochiai S, Osamura K, Waku Y and Yamamura T, J. Jpn. Inst. Met, 57, 1035-1040, 1993.